Journal Pre-proofs

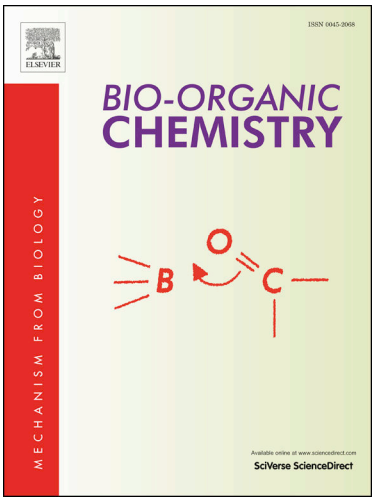

Design, Synthesis, Cytotoxicity Screening and Molecular Docking of New 3-Cyanopyridines as Survivin inhibitors and Apoptosis Inducers

Rehab Sabour, Marwa F. Harras, Ahmed B.M. Mehany

PII: S0045-2068(19)30324-4
DOI: https://doi.org/10.1016/j.bioorg.2019.103358
Reference: YBIOO 103358

To appear in: *Bioorganic Chemistry*

Received Date: 26 February 2019
Revised Date: 23 September 2019
Accepted Date: 9 October 2019

Please cite this article as: R. Sabour, M.F. Harras, A.B.M. Mehany, Design, Synthesis, Cytotoxicity Screening and Molecular Docking of New 3-Cyanopyridines as Survivin inhibitors and Apoptosis Inducers, *Bioorganic Chemistry* (2019), doi: https://doi.org/10.1016/j.bioorg.2019.103358

Design, Synthesis, Cytotoxicity Screening and Molecular Docking of New 3-Cyanopyridines as Survivin inhibitors and Apoptosis Inducers

Rehab Sabour[a], Marwa F. Harras[a*] and Ahmed B. M. Mehany[b]

[a] Department of Pharmaceutical Chemistry, Faculty of Pharmacy (Girls), Al-Azhar University, Cairo, Egypt [b] Department of Zoology, Faculty of Science (Boys), Al-Azhar University, Cairo, Egypt

Abstract

Recently, targeting survivin proved to be an attractive strategy for developing anticancer agents. Survivin overexpression is highly correlated with cancer aggressiveness, recurrence and resistance to chemotherapeutic treatment and radiotherapy. Additionally, survivin is overexpressed selectively in most cancer types with a very little expression in completely differentiated cells, which encouraged us to design and synthesize a novel series of 3-cyanopyridine derivatives targeting survivin. The newly synthesized compounds were evaluated for their cytotoxic activities against three cancer cell lines; PC-3, HepG2 and MDA-MB-231. Compounds **4a, 4b, 5c** and **6c** showed significant cytotoxic activities that were more potent than the reference drug, 5-FU. Hence, these compounds were selected to be further studied regarding their apoptotic potential in PC-3 cells. Interestingly, they decreased the level of Bcl-2 by 1.9-3.8 folds and increased the level of Bax by 6.1-8.8 folds compared to the control. Moreover, they elevated the level of active caspase-3 by 7.1-8.5 folds in comparison to the control. In order to estimate the cytotoxicity level of these compounds in non-tumorigenic cells, WI38 cells were treated with these compounds. They showed high IC_{50} values (148.57-193.64 μM), indicating selective cytotoxicity to the tumor cells, and much less toxic effect to the normal ones. Additional studies on the mechanism of **4a**, the most active compound, revealed that it induced cell cycle arrest at the G2/M phase in addition to an increase in the percentage of pre-G1 apoptotic cells. Furthermore, western blotting was carried out using different concentrations of **4a**. Results showed that **4a** markedly suppressed survivin expression in PC-3 cells and caused a decrease in the caspase-7/cleaved caspase-7 ratio and in Bcl-2/Bax ratio, in addition to an increase in the level of the cleaved PARP. Finally, docking study of the most active compound in the active site (dimerization site) of survivin was in agreement with the *in vitro* survivin inhibitory activity.

Keywords: Cyanopyridine; synthesis; anticancer; cell cycle; apoptosis; survivin

1. Introduction

Cancer is a disease where important mechanisms of the cell cycle are dysfunctional, associated with either an over reproduction and/or decreased elimination of cells [1]. Physiological processes are organized by a balance between cellular proliferation, differentiation and apoptosis [2]. Programmed cell death (apoptosis), is a dynamic process that can be stimulated by DNA-damaging agents such as radiation and chemotherapeutic drugs. Studies have shown a great relationship between increased resistance to anticancer drugs and decreased capability to undergo apoptosis [3]. Accordingly, susceptibility to apoptosis is an important determinant of response to anti-neoplastic therapy [4]. Therefore, suppression of apoptosis throughout carcinogenesis is supposed to play a principal role in the progression of cancer. There are different types of molecular mechanisms that cancer cells use to suppress apoptosis. They acquire resistance to apoptosis via the expression of anti-apoptotic proteins such as Bcl-2 and survivin or by down-regulation of different caspases and pro-apoptotic proteins such as Bax [5]. The relation between pro-apoptotic and anti-apoptotic levels is an important determinant of cell survival [2].

The anti-apoptotic protein (survivin) is one of the inhibitors of apoptosis family, which is expressed in the G2/M phases of the cell cycle almost solely in cancer cells, but absent in most normal adult differentiated tissues. It promotes the survival of cancer cells through suppression of caspase-mediated apoptosis [6-12]. Overexpression of survivin is positively correlated with cancer cell resistance to chemotherapy and poor patient prognosis. Therefore, survivin is considered one of the important targets aiming to produce new candidates of promising anticancer activity [13, 14].

By searching literatures for chemical scaffolds effective as survivin inhibitors, we found that 2-oxo-3-cyanopyridine derivative **I** has significant anti-survivin activity [15]. Hence great interest has been focused on 3-cyanopyridine scaffold owing to the notable anticancer activity against a wide range of cell lines [16-19]. Interestingly different members belonging to this scaffold have been shown promising activity through interfering survivin [20]. Furthermore, some derivatives of 2-oxo-3-cyanopyridine with higher lipophilic properties can inhibit survivin [17]. Thus, our structure-based design strategy is originated on structural modification of compound **I**. This is achieved via sparing the pharmacophoric group responsible for survivin inhibition, 3-

cyanopyridine group, and incorporating benzyloxy moiety at 6- position in order to exert more lipophilic character to the compound, while substituting the 2- and 4- positions with different moieties (**Fig.1**).

To explore the scope of this class of compounds, a novel series of 3-cyanopyridine was designed and synthesized. All of the newly synthesized compounds were evaluated for their anticancer activity against three cell lines; prostate cancer cell line (PC-3), liver cancer cell line (HepG2) and breast cancer cell line (MDA-MB-231). Apoptotic studies were applied in order to estimate the potential of the most potent compounds to induce apoptosis. Therefore, promising compounds were evaluated for their effect on the level of some apoptosis key markers (Bcl-2, Bax, caspase-3). Cell cycle analysis and Western blotting were carried out to confirm our findings. Moreover, a molecular docking study was done to find out the probable binding interactions of the most active compounds with survivin.

2. Results and discussion

2.1. Chemistry

Scheme 1 outlines the steps used for the synthesis of the target compounds. In this work, chalcones **3a-d** were prepared as reported by condensation of benzyloxyacetophenone (**1**) with different acetophenones **2a-d** in the presence of NaOH [21]. The condensation reaction of **3a-d** with malononitrile in ethanol containing ammonium acetate [22] afforded the target 2-amino-3-cyanopyridine derivatives **4a-d.** The structures of compounds **4a-d** were well established on the basis of their micro-analytical analysis and spectral data. IR spectrum of compound **4b**, taken as a representative example of this series, showed absorption bands at 3296, 3142 cm^{-1} corresponding to the NH_2 function and a sharp band at 2216 cm^{-1} for the nitrile group. Its ^{1}HNMR spectrum (DMSO-d6) revealed the presence of singlet at 5.18 ppm for the O-CH_2 protons and a singlet at 6.76 ppm due to H-5 of the pyridine ring, in addition to a singlet at δ 9.79 ppm for NH_2 protons (exchangeable with D_2O).

On the other hand, chalcones **3a-d** were condensed with 2-cyanoacetamide and 2-cyanothioacetamide in ethanol in the presence of pipridine [23] to produce 3-cyanopyridine-2-ones **5a-d** and 3-cyanopyridine-2-thiones **6a-d**, respectively. The proposed structures of these compounds were supported by elemental and spectral measurements. IR spectra of compounds **5a-d** and **6a-d** displayed absorption bands at 3200-3434 cm^{-1} assigned to NH groups besides the

appearance of absorption bands at 2205-2217 cm^{-1} comprising the nitrile group. Moreover, for compounds **5a-d**, the carbonyl function appeared as absorption bands around 1640 cm^{-1}. ^{1}HNMR spectra **5a-d** and **6a-d** revealed the presence of singlet signals at 5.12-5.23 ppm corresponding to the O-CH_2 protons and singlet signals at 6.60-6.95 ppm representing H-5 of the pyridine ring.

2.2. Biological evaluation

2.2.1. In vitro cytotoxic activity

The *in vitro* cytotoxicity of the synthesized compounds **4a-d, 5a-d** and **6a-d** was evaluated against a panel of cell lines, namely; the prostate cancer cell line (PC-3), the liver cancer cell line (HepG2) and the breast cancer cell line (MDA-MB-231). 5-FU, being broadly used in cancer managing, was used as the reference drug. The results were represented as IC_{50} values and shown in **(Table 1)**. Interestingly, **4a** was the most potent 3-cyanopyridine derivative. It showed 17.92 times the activity of 5-FU against PC-3 cell line, 6.68 times against HepG2 and 11.75 times against MDA-MB-231.

The screening results indicated that most of the tested compounds have excellent anti-proliferative activity against PC-3 cell line. This is demonstrated by the IC_{50} values of compounds **4a,b,d**, **5b-d** and **6a-d** (IC_{50} = 0.42- 9.83 μM) which were more active than 5-FU (IC_{50} = 7.53 μM). While compounds 4c and 5a displayed moderate activity (IC_{50} = 9.83 and 14.71 μM, respectively).

Scanning the IC_{50} values of the tested compounds against HepG2 cell line revealed that most of the compounds exert good to moderate cytotoxic influence. Compounds **4a,b**, **5c** and **6b,c** (IC_{50} = 1.22- 6.92 μM) were found to be more potent than 5-FU (IC_{50} = 8.15 μM). On the other hand, compounds **4c,d**, **5a,b,d** and **6a,d** showed moderate activity (IC_{50} = 10.64- 21.35 μM).

Regarding the anticancer activity of the target compounds against MDA-MB-231breast cell line, Compounds **4a,b**,**d 5b,c** and **6a-d** displayed good antitumor activity (IC_{50} = 0.66- 9.34 μM) compared to the reference drug (IC_{50} = 9.35 μM). While the rest of the compounds exhibited moderate cytotoxicity (IC_{50} = 10.71- 18.38 μM).

Furthermore, in order to estimate the safety on normal cells, the most active compounds **4a, 4b, 5c** and **6c** were further screened on non-cancerous human WI-38 cells. It was found that these compounds are selective cytotoxic agents on the cancer cells and much less toxic on the normal

cells WI-38 as demonstrated from their IC_{50} values (193.15, 193.64, 169.32 and 148.57 μM, respectively) (**Table 2**)

Compounds **4a, 4b, 5c** and **6c,** exhibiting significant and selective cytotoxic effects, were chosen to be further studied regarding their potential to induce apoptosis in PC-3 cells.

2.2.2. Apoptosis studies

Apoptosis is the physiologically important way of programmed cell death that compensates cell growth and tissue homeostasis in the normal prostate gland [24]. The ability of **4a, 4b, 5c** and **6c** to induce apoptosis in PC-3 cells was estimated by observing the levels of some apoptosis key markers; Bcl-2, Bax and active caspase-3 that give clear evidence for apoptosis induction.

2.2.2.1. *Effects on the levels of Bax and Bcl-2 proteins*

Apoptosis is regulated by different factors including the Bcl-2 family: suppressors (Bcl-2 protein), inducers (Bax protein) and by stimulation of the apoptotic pathway through caspase-3 [25]. Many studies on human cancers have revealed the presence of a relationship between increased levels of Bcl-2, decreased levels of Bax and uncontrolled cell growth [24,26]. Here, the levels of Bcl-2 and Bax after treatment of PC-3 cells with **4a, 4b, 5c** and **6c** were determined. The results as illustrated in **Table 3** demonstrated that **4a, 4b, 5c** and **6c** decreased the level of Bcl-2 by 3.8, 2.3, 3.3 and 1.9 folds, respectively and increased the level of Bax by 8.8, 7.2, 7.7 and 6.1 folds, respectively compared to the control. These results indicated that these compounds moved the prostate cancer cells towards apoptosis.

2.2.2.2. Effects on the level of active caspase-3

The principal constituents of apoptotic pathways are the caspase family of cysteine proteases [24]. Up to now, several earlier studies have proved that caspase-3 is an executioner of apoptosis and that its activation results in the induction of apoptosis [25,27]. In this study, PC-3 cells were treated with compounds **4a, 4b, 5c** and **6c** and the level of caspase-3 was determined. Results revealed that the active caspase-3 was significantly overexpressed by 8.5, 7.2, 7.5 and 7.1 folds, respectively compared to the control indicating the apoptosis induction potential of these compounds (**Table 3**).

2.2.3. Cell cycle analysis:

The mechanism of the cytotoxic effect of many antitumor agents involves the combination of induction of apoptosis together with cell cycle arrest [28, 29]. Furthermore, regulation of the cell cycle and induction of apoptosis are suggested to be effective methods in the development of anticancer therapeutics [30]. Thus, it was significant to know if the arrest of the cell cycle was a part of the cytotoxic mechanism of our most active compound **4a**. Flow cytometry analysis was done on PC-3 cells after incubation with **4a** for 24 h and the results were shown in **Fig. 2**. The outcome proposed that **4a** could induce cell cycle arrest in the G2/M phase as it increased the DNA content in G2/M phase by 3.1 folds with subsequent reduction in G0/G1 and S phases compared to the control cells. Moreover, it caused a notable increase in the amount of pre-G1 apoptotic cells.

The apoptotic effect of **4a** was further estimated by Annexin V-FITC assay. As displayed in **Fig. 3**, the total apoptotic cells percentage significantly increased after treatment by this compound indicating the capability of **4a** to induce apoptosis which were consistent with the previous results.

2.2.4. Western blotting:

Survivin is a proto-oncogene biomarker known for its anti-apoptotic properties. Increased expression of survivin is associated with a decrease in the overall survival in cancer patients [31]. To determine whether our new compound **4a** causes survivin degradation, western blotting analysis was performed in PC-3 cell line using different concentrations of **4a**. As shown in **Fig. 4-A**, **4a** markedly inhibited survivin expression in PC-3cells in a concentration dependent manner. Moreover, **Fig. 4-B** displayed the effect of **4a** on the expression of caspase-7 and cleaved caspase-7 and showed that **4a** caused a significant increase of cleaved caspase-7 with a subsequent decrease in the caspase-7/cleaved caspase-7 ratio. In addition, the apoptosis inhibitor Bcl-2 expression was effectively decreased, while the apoptosis inducer Bax protein expression was increased as shown in **Fig. 4-C**.

PARP (poly ADP-ribose polymerase), the substrate of caspases, is cleaved during apoptosis by caspases. [32]. Consistent with survivin inhibition, **4a** elevated the level of cleaved PARP (PARP 85 KD) as a further indication of the apoptosis induction potential of this compound (**Fig. 4-D**).

2.3. Molecular docking study

In most cancer cells survivin exists as a homodimer, which is considered necessary for its physiological function. Destabilization and degradation of the protein is encouraged by targeting of the small molecule into a domain that interfere with the dimerization hydrophobic interface, thereby further leading to cancer cells apoptosis [33].

To understand the obtained biological data on a structural basis, compound **I** together with the most active compound; **4a** were evaluated through docking techniques (**Table 4**). In the present study, the ligand-receptor interactions of both compounds with (survivin) were investigated by performing docking studies using Molecular Operating Environment (MOE). The X-ray crystal structure of the survivin protein (PDB code 3UIH) was obtained from the Protein Databank.

Docking of compound **I** with survivin showed marked binding interaction with binding energy -6.79 Kcal/mol, the apparent H-bonding resulted from the interaction of the NH group of the pyridine ring with the catalytic residue Gln92. Additionally, the phenolic oxygen made H-bonding interaction with Glu40. Furthermore, arene-cation interaction was observed between the substituted phenolic group at position 6 of the pyridine ring and Arg18 amino acid (**Fig. 5**).

Docking study of compound **4a** (**Fig. 6**) showed that it was able to fit in the binding pocket of survivin with higher binding energy - 8.478 Kcal/mol,

Results obtained indicated that **4a** exhibited strong interactions forming appealing hydrogen bonding and π-π stacking interactions with the survivin protein that include: (1) H-bonding interaction between nitrogen atom of NH_2 group at position 2 of the pyridine ring and the side chain acidic group of Glu40; (2) H-bonding interaction between the cyano group and the side chain basic group of Arg18; (3) H-bonding interaction between the cyano group and the side chain of Lys15; (4) π-π stacking interaction between the phenyl ring at position 4 of the pyridine ring and residue Phe93.

Moreover compounds **4b**, **5c** and **6c** displayed high binding affinities with very close binding modes in the survivin active site (**Fig. 7**).

Additionally, the docking of protein-protein interactions of chain A and chain B wild-type and complex-type were carried out to predict affinity and survivin binding free energy (ΔG). The wild-type ΔG was found to be -59.3 kcal/mol, while the complex-type displayed higher ΔG value (-58.7 kcal/mol). The complex dimer has rmsd value of 0.47 Å relative to wild-type dimer.

Furthermore, docking study was done to show the affinity of **4a** for some other BIR domain containing proteins (XIAP-BIR2 (PDB code 1I3O, chain E) and ML-IAP (PDB code 3f7g, chain E) and they showed lower binding affinities with binding scores ranging from -3 to -2 Kcal/mol).

2.4. Molecular dynamic simulation

Molecular dynamic simulation was performed in this study in order to understand the dynamics of survivin interaction sites. The results are reported in **Table 5** which include the amino acid residues involved in interface binding of wild-type and the amino acid residues which is disrupted in wild-type and involved in ligand complex.

Crystallographic studies have indicated that survivin forms homodimers across the interface (the amino acid residues of 6-10, 89-102) of dimerization [8,34], which is mediated by protein-protein interactions. The dimerization is stabilized by several typical interactions. However, these interactions are supposed to be broken or disrupted during docking of chemical compounds, these are:

A. The backbone amino acid residues of Glu94, Leu96, Leu98 and Gly99 which interacted by hydrogen bonding interactions between chain A and chain B and these interactions remain unchanged during the molecular dynamic simulations of the docked compound. (**Fig. 8**).
B. Aromatic stacking network interactions between Trp10, and Phe101 located in the dimerization interface, which suggested to form intramolecular constraint to keep survivin in dimer form or alternatively to be disrupted in ligand binding site conformation that destabilize surviving dimer [8,34]. As shown in **Fig. 9**, Trp10 of chain A is involved in aromatic network stacking interactions with Trp10 of chain B and Phe101 in wild-type conformation. However, upon docking, the interaction between Trp10 of chain A and Trp10 of chain B is disorganized as Trp10 of chain A (docked form) is rotated inside the chain A to stabilize complex conformation by forming hydrogen bonding mediated interactions between Trp10, Arg108, and Asp105.
C. Hydrogen bonding interaction of Thr5 and Asp105 between chain A and chain B. respectively is essential for survivin protein-protein interactions. However, in complex conformation, the network of hydrogen bonding interactions is formed among Phe58,

Asp105, Arg108, Trp10, and Ala9 (**Fig. 10**). This network is suggested to stabilize the complex via enhancing the aromatic stacking interaction between the ligand and Phe58.

D. The dimeric structure is stabilized by the formation of hydrophobic interactions between Phe93 and Leu98 which are considered core residues of the dimerization interface [35] and a common feature in survivin protein-protein interactions. While, in case of complex, Phe93 facilitates complex binding by forming hydrophobic interaction with the ligand (**Fig. 11**). Moreover it was found that the ligand formed hydrophobic interaction with leu96, and phe101.

Results analysis indicated that characteristic differences between the wild-type and complex conformation, which correlated well with published results.

This modeling study revealed that **4a** restricts the dimerization hydrophobic domain of survivin which was in agreement with western plotting analysis that showed that **4a** can considerably decrease the amount of survivin in PC-3 cells, proving the possible proposed mechanism in the molecular docking. Moreover, high selectivity of **4a** on cancer cells versus normal cells further supported our suggested mechanism of inhibiting the function of survivin protein that is mainly expressed in cancer cells.

3. Conclusion

Based on the structural features of the survivin inhibitor **I**, a novel series of 3-cyanopyridines were designed and synthesized. Their cytotoxic activities against PC-3, HepG2 and MDA-MB-231 cell lines were investigated through MTT screening. Most of the new compounds exhibited high *in vitro* anticancer activities, especially against the prostatic PC-3 cell line. The best activities were observed in **4a, 4b, 5c** and **6c**. These compounds were subjected to apoptosis studies in order to estimate their apoptotic potentials. They caused a decrease in the expression of the apoptosis suppressor Bcl-2 and an increase in the level of apoptosis inducer Bax in addition to increasing the amount of active caspase-3. Cell cycle analysis of the most potent compound **4a** revealed cell cycle arrest at the G2/M phase with an increase in the amount of pre-G1 apoptotic cells as a further indication of apoptosis potential of this compound. Additionally, western blotting analysis was carried out in PC-3 cell line and the results indicated that **4a** caused potent suppression in the expression of survivin protein. At last, molecular docking study showed that **4a** can fit the survivin active site with a higher binding score than the inhibitor **I**.

4. Experimental

All chemicals were purchased from VWR International Merck, Germany or Sigma-Aldrich and used without further purification. Melting Points were carried out by open capillary tube method using Stuart SMP3 Melting Point apparatus and they are uncorrected. Elemental Microanalysis was carried out at the Regional Center for Mycology and Biotechnology, Al-Azhar University. Infrared spectra were recorded using potassium bromide discs on Schimadzu FT/IR 1650 (Perkin Elmer) at the faculty of science, Al-Azhar University. ^{1}HNMR and ^{13}CNMR Spectra were recorded on a Varian Gemini 300 MHz Spectrophotometer, the spectra were run at 300 MHz in deuterated dimethylsulfoxide (DMSO-d6) at the Armed Forces Laboratories or on Agilent Technologies 400 MHz NMR spectrophotometer at Microanalytical Unit, faculty of pharmacy, Cairo University. Chemical shifts were expressed in δ units and were related to that of the solvents. As for the proton magnetic resonance, D_2O was carried out for NH and OH exchangeable protons. Mass Spectra were recorded using Shimadzu Gas Chromatograph Mass spectrometer-Qp 2010 plus (Japan) at the Regional Center for Mycology and Biotechnology, Al-Azhar University. All the reactions were followed by thin layer chromatography using silica gel F254 plates (Merck) and were visualized by UV-lamp. 1-(4-(benzyloxy)phenyl)ethanone (**1**) was prepared according to reported procedure [36], chalcones **3a-d** were prepared as reported [37,38].

4.1. *Synthesis*

*4.1.1. General procedure for the synthesis of compounds **4a-d***

A mixture of chalcones **3a-d** (3 mmol), malononitrile (0.2 g, 3 mmol) and ammonium acetate (0.7 g, 9 mmol) in 20 ml absolute ethanol was heated under reflux for 8 hours during which the product was separated out. Then the reaction mixture was cooled and the precipitate was filtered, washed with cold ethanol, air dried and crystallized from ethanol.

2-amino-6-(4-(benzyloxy)phenyl)-4-phenylnicotinonitrile (**4a**)

Yield 65%; m.p. 125-127 ^{o}C; IR (KBr, cm^{-1}): 3248, 3197 (NH_2), 3067 (CH aromatic), 2935 (CH aliphatic), 2216 (CN), 1604 (C=C &C=N); ^{1}HNMR (DMSO-d6) δ (ppm): 5.19 (s, 2H, OCH_2),

7.08-7.45 (m, 7H, 7 aromatic H), 7.71 (s, 1H, CH of pyridine), 7.85-8.17 (m, 7H, 7 aromatic H), 10.19 (2H, NH_2; exchangeable with D_2O); ^{13}CNMR (DMSO-d6) δ (ppm): 69.98, 90.75, 115.12 , 115.21 (2C), 122.47, 128.27 (2C), 128.48 (2C), 128.72 (2C), 128.95 (2C), 129.24 (2C), 129.63, 130.91, 131.04, 136.95, 138.29, 143.63, 162.41, 162.78, 162.96; MS, m/z: 377 (M^+, 1.42%); Anal. Calcd. For $C_{25}H_{19}N_3O$ (377.44): C, 79.55; H, 5.07; N, 11.13, Found: C, 79.82; H, 5.21; N, 11.28.

2-amino-6-(4-(benzyloxy)phenyl)-4-(4-fluorophenyl)nicotinonitrile (**4b**)
Yield 57%; m.p. 140-42 ^oC; IR (KBr, cm^{-1}): 3296, 3142 (NH_2), 3032 (CH aromatic), 2931 (CH aliphatic), 2216 (CN), 1601 (C=C &C=N); ^{1}HNMR (DMSO-d6) δ (ppm): 5.18 (s, 2H, OCH_2), 6.76 (s, 1H, CH of pyridine), 7.04-7.92 (m, 13H, 13 aromatic H), 9.79 (2H, NH_2; exchangeable with D_2O); ^{13}CNMR (DMSO-d6) δ (ppm): 69.88, 81.07, 115.11, 115.58 (2C), 116.13 (2C), 128.02, 128.21 (2C), 128.43 (2C), 128.86 (2C), 128.94, 129.59 (2C), 129.86, 130.63, 131.24, 133.25, 137.07, 161.13, 162.38, 164.85; MS, m/z: 395 (M^+, 45.77%); Anal. Calcd. For $C_{25}H_{18}FN_3O$ (395.43): C, 75.93; H, 4.59; N, 10.63, Found: C, 76.12; H, 4.70; N, 10.89.

2-amino-6-(4-(benzyloxy)phenyl)-4-(4-chlorophenyl)nicotinonitrile (**4c**)
Yield 68%; m.p. 102-104 ^oC; IR (KBr, cm^{-1}): 3350, 3222 (NH_2), 3064 (CH aromatic), 2977 (CH aliphatic), 2212 (CN), 1595 (C=C &C=N); ^{1}HNMR (DMSO-d6) δ (ppm): 5.22 (s, 2H, OCH_2), 7.12 (d, 1H, aromatic H), 7.33 (s, 1H, CH of pyridine), 7.34-7.98 (m, 13H, 13 aromatic H), 8.20 (2H, NH_2; exchangeable with D_2O); ^{13}CNMR (DMSO-d6) δ (ppm): 70.00, 87.38, 113.54, 113.82 (2C), 115.24, 127.60, 128.25 (2C), 128.50 (2C), 128.82 (2C), 128.97 (2C), 129.45, 129.58 (2C), 130.65, 130.94, 133.38, 136.88, 161.00, 162.13, 163.02; MS, m/z: 413 [$(M+2)^+$, 3.46%], 411 (M^+, 1.36%); Anal. Calcd. For $C_{25}H_{18}ClN_3O$ (411.88): C, 72.90; H, 4.40; N, 10.20, Found: C, 73.12; H, 4.57; N, 10.48.

2-amino-6-(4-(benzyloxy)phenyl)-4-(thiophen-2-yl)nicotinonitrile (**4d**)
Yield 72%; m.p. 225-227 ^oC; IR (KBr, cm^{-1}): 3307, 3212 (NH_2), 3102 (CH aromatic), 2925 (CH aliphatic), 2216 (CN), 1600 (C=C &C=N); ^{1}HNMR (DMSO-d6) δ (ppm): 5.22 (s, 2H, OCH_2), 7.00 (s, 1H, CH of pyridine), 7.04-8.12 (m, 12H, 9 aromatic H+ 3H of thiophene), 8.35 (2H, NH_2; exchangeable with D_2O); ^{13}CNMR (DMSO-d6) δ (ppm): 70.03, 84.51, 113.49, 113.82,

115.29 (2C), 126.45 (2C), 127.58 (2C), 128.27, 128.51 (2C), 128.98 (2C), 129.50, 130.66, 130.98, 136.87, 140.58, 161.5, 162.66, 163.08; MS, m/z: 383 (M^+, 0.88%); Anal. Calcd. For $C_{23}H_{17}N_3OS$ (383.47): C, 72.04; H, 4.47; N, 10.96, Found: C, 72.31; H, 4.64; N, 11.23.

*4.1.2. General procedure for the synthesis of compounds **5a-d** and **6a-d***

A mixture of chalcones **3a-d** (3 mmol) and cyanoacetamide/ cyanothioacetamide (3 mmol) in 20 ml absolute ethanol containing few drops of piperdine was refluxed for 6 hours, allowed to cool, poured on ice-cold water and acidified with HCl. The solid formed was filtered and recrystallized from ethanol.

*6-(4-(benzyloxy)phenyl)-2-oxo-4-phenyl-1,2-dihydropyridine-3-carbonitrile (**5a**)*

Yield 74%; m.p. 154-156 ^oC; IR (KBr, cm^{-1}): 3284 (NH), 3061 (CH aromatic), 2952 (CH aliphatic), 2215 (CN), 1638 (CO), 1570 (C=C); ^{1}HNMR (DMSO-d6) δ (ppm): 5.22 (s, 2H, OCH_2), 6.78 (s, 1H, CH of pyridine), 7.15-7.92 (m, 14H, aromatic H), 12.69 (1H, NH; exchangeable with D_2O); ^{13}CNMR (DMSO-d6) δ (ppm): 69.92, 115.60 (2C), 115.83, 123.22, 127.12 (2C), 128.24, 128.46 (2C), 128.68 (2C), 128.97, 129.22 (2C), 129.93 (2C), 130.75 (2C), 136.54, 137.09, 151.89, 158.76, 161.22, 163.20; MS, m/z: 378 (M^+, 100.00%); Anal. Calcd. For $C_{25}H_{18}N_2O_2$ (378.42): C, 79.35; H, 4.79; N, 7.40, Found: C, 79.48; H, 4.87; N, 7.67.

6-(4-(benzyloxy)phenyl)-4-(4-fluorophenyl)-2-oxo-1,2-dihydropyridine-3-carbonitrile (**5b**)

Yield 58%; m.p. 260-262 ^oC; IR (KBr, cm^{-1}): 3200 (NH), 3071 (CH aromatic), 2945 (CH aliphatic), 2217 (CN), 1640 (CO), 1571 (C=C); ^{1}HNMR (DMSO-d6) δ (ppm): 5.19 (s, 2H, OCH_2), 6.65 (s, 1H, CH of pyridine), 7.12-7.89 (m, 13H, aromatic H), 8.10 (1H, NH; exchangeable with D_2O); ^{13}CNMR (DMSO-d6) δ (ppm): 69.91, 105.91, 115.30 (2C), 115.65, 116.33, 128.21 (2C), 128.44, 128.56 (2C), 128.95 (2C), 129.95 (2C), 131.20 (2C), 130.39, 131.29, 133.03, 133.06, 137.04, 160.26, 162.45, 164.92; MS, m/z: 396 (M^+, 100.00%); Anal. Calcd. For $C_{25}H_{17}FN_2O_2$ (396.41): C, 75.75; H, 4.32; N, 7.07, Found: C, 76.01; H, 4.45; N, 7.24.

6-(4-(benzyloxy)phenyl)-4-(4-chlorophenyl)-2-oxo-1,2-dihydropyridine-3-carbonitrile (**5c**)

Yield 81%; m.p. 245-247 ^oC; IR (KBr, cm^{-1}): 3383 (NH), 3067 (CH aromatic), 2936 (CH aliphatic), 2205 (CN), 1641 (CO), 1600 (C=C); ^{1}HNMR (DMSO-d6) δ (ppm): 5.14 (s, 2H,

OCH_2), 6.60 (s, 1H, CH of pyridine), 7.02-7.98 (m, 13H, aromatic H), 10.00 (1H, NH; exchangeable with D_2O); ^{13}CNMR (DMSO-d6) δ (ppm): 69.80, 103.69, 112.44 (2C), 114.90, 115.42, 128.19 (2C), 128.39, 128.90 (2C), 128.95 (2C), 129.24 (2C), 129.38 (2C), 130.39, 133.82, 134.64, 136.85, 137.30, 150.94, 160.05, 164.19; MS, m/z: 414 [$(M+2)^+$, 1.87%], 412 (M^+, 5.03%); Anal. Calcd. For $C_{25}H_{17}ClN_2O_2$ (412.87): C, 72.73; H, 4.15; N, 6.79, Found: C, 72.96; H, 4.37; N, 6.94.

6-(4-(benzyloxy)phenyl)-2-oxo-4-(thiophen-2-yl)-1,2-dihydropyridine-3-carbonitrile (**5d**) Yield 64%; m.p. 135-137 ^{o}C; IR (KBr, cm^{-1}): 3434 (NH), 3178 (CH aromatic), 2950 (CH aliphatic), 2206 (CN), 1641 (CO), 1587 (C=C); ^{1}HNMR (DMSO-d6) δ (ppm): 5.21 (s, 2H, OCH_2), 6.94 (s, 1H, CH of pyridine), 7.01-7.47 (m, 7H, 7 aromatic H), 7.57 (1H, NH; exchangeable with D_2O), 7.65-8.09 (m, 5H, 2 aromatic H+ 3H of thiophene); ^{13}CNMR (DMSO-d6) δ (ppm): 70.00, 105.17, 115.30 (2C), 120.79, 125.69, 127.81, 128.27 (2C), 128.91, 128.95 (2C), 129.11 (2C), 130.60, 131.21, 132.93, 136.37, 136.75, 140.29, 144.53, 162.72, 163.18; MS, m/z: 384 (M^+, 41.29%); Anal. Calcd. For $C_{25}H_{16}N_2O_2S$ (384.45): C, 71.85; H, 4.19; N, 7.29, Found: C, 72.01; H, 4.36; N, 7.48.

6-(4-(benzyloxy)phenyl)-4-phenyl-2-thioxo-1,2-dihydropyridine-3-carbonitrile (**6a**) Yield 83%; m.p. 203-205 ^{o}C; IR (KBr, cm^{-1}): 3208 (NH), 3056 (CH aromatic), 2938 (CH aliphatic), 2213 (CN), 1569 (C=C); ^{1}HNMR (DMSO-d6) δ (ppm): 5.12 (s, 2H, OCH_2), 6.73 (1H, NH; exchangeable with D_2O), 6.85 (s, 1H, CH of pyridine), 7.01-8.09 (m, 14H, 14 aromatic H); ^{13}CNMR (DMSO-d6) δ (ppm): 69.86, 102.61, 115.57 (2C), 128.20 (2C), 128.43, 128.92 (2C), 129.26 (2C), 129.42 (3C), 129.71, 129.89 (2C), 130.76, 130.98, 131.06, 137.01, 154.89, 158.89, 161.25, 165.65; MS, m/z: 394 (M^+, 100.00%); Anal. Calcd. For $C_{25}H_{18}N_2OS$ (394.49): C, 76.12; H, 4.60; N, 7.10, Found: C, 76.01; H, 4.79; N, 7.36.

6-(4-(benzyloxy)phenyl)-4-(4-fluorophenyl)-2-thioxo-1,2-dihydropyridine-3-carbonitrile (**6b**) Yield 55%; m.p. 110-112 ^{o}C; IR (KBr, cm^{-1}): 3202 (NH), 3065 (CH aromatic), 2935 (CH aliphatic), 2207 (CN), 1568 (C=C); ^{1}HNMR (DMSO-d6) δ (ppm): 5.19 (s, 2H, OCH_2), 5.82 (1H, NH; exchangeable with D_2O), 6.95 (s, 1H, CH of pyridine), 7.06-8.27 (m, 13H, aromatic H); ^{13}CNMR (DMSO-d6) δ (ppm): 69.83, 91.49, 110.91, 115.02 (2C), 115.47 (2C), 115.97, 121.05,

128.21 (2C), 128.89 (2C), 129.42 (2C), 130.40 (2C), 130.98, 131.79, 137.24, 151.40, 155.80, 157.32, 160.72, 162.80; MS, m/z: 412 (M^+, 33.73%); Anal. Calcd. For $C_{25}H_{17}FN_2OS$ (412.48): C, 72.80; H, 4.15; N, 6.79, Found: C, 73.04; H, 4.31; N, 6.88.

6-(4-(benzyloxy)phenyl)-4-(4-chlorophenyl)-2-thioxo-1,2-dihydropyridine-3-carbonitrile (**6c**) Yield 75%; m.p. 233-235 ^oC; IR (KBr, cm^{-1}): 3203 (NH), 3067 (CH aromatic), 2939 (CH aliphatic), 2214 (CN), 1573 (C=C); ^{1}HNMR (DMSO-d6) δ (ppm): 5.23 (s, 2H, OCH_2), 6.74 (s, 1H, CH of pyridine), 6.82 (1H, NH; exchangeable with D_2O), 7.14-8.27 (m, 13H, aromatic H); ^{13}CNMR (DMSO-d6) δ (ppm): 69.91, 101.16, 115.58 (2C), 116.05, 124.87, 128.23 (2C), 128.41 (2C), 128.94, 129.37 (2C), 129.79 (2C), 130.01 (2C), 131.03, 135.40, 137.22, 153.39, 158.31, 161.06, 165.32, 167.54; MS, m/z: 430 [$(M+2)^+$, 2.76%], 428 (M^+, 8.41%); Anal. Calcd. For $C_{25}H_{17}ClN_2OS$ (428.93): C, 70.00; H, 3.99; N, 6.53, Found: C, 69.89; H, 4.16; N, 6.74.

6-(4-(benzyloxy)phenyl)-4-(thiophen-2-yl)-2-thioxo-1,2-dihydropyridine-3-carbonitrile (**6d**) Yield 58%; m.p. 228-230 ^oC; IR (KBr, cm^{-1}): 3177 (NH), 3064 (CH aromatic), 2936 (CH aliphatic), 2205 (CN), 1566 (C=C); ^{1}HNMR (DMSO-d6) δ (ppm): 5.17 (s, 2H, OCH_2), 6.74 (s, 1H, CH of pyridine), 6.89 (1H, NH; exchangeable with D_2O), 7.13-8.26 (m, 12H, 9 aromatic H+ 3H of thiophene); ^{13}CNMR (DMSO-d6) δ (ppm): 69.86, 98.76, 109.92, 115.43 (2C), 115.52, 118.70, 128.22 (2C), 128.43, 128.82 (2C), 128.94 (2C), 129.38, 130.29, 130.36, 137.09, 137.23, 157.49, 160.78, 163.52, 166.23; MS, m/z: 400 (M^+, 84.40%); Anal. Calcd. For $C_{23}H_{16}N_2OS_2$ (400.52): C, 68.97; H, 4.03; N, 6.99, Found: C, 69.20; H, 4.18; N, 7.23.

4.2. *Biological evaluation*

4.2.1. *In vitro* anti-tumor assay

4.2.1.1. Methodology: cell culture

Cancer cell lines; Human prostate carcinoma cell lines (PC-31), hepatocellular carcinoma cell lines (HEPG-2) and human breast adenocarcinoma cell line (MDA-MB-231) and normal cell line (WI-38) were obtained from American Type Cell Culture Collection (ATCC, Manassas, USA) and grown on the appropriate growth medium Dulbecco's modified Eagle's medium (DMEM/ Life Technologies) supplemented with 10% FBS (fetal bovine serum) (Hyclone), 10 ug/ml of insulin (Sigma) and 1% penicillin-streptomycin. All of the other chemicals and reagents were

from Sigma or Invitrogen. Plate cells (cells density 1.2 – 1.8 × 10,000 cells/well) in a volume of 100 µl complete growth medium + 100 ul of the tested compound per well in a 96-well plate for 24 h before the MTT assay.

4.2.1.2. MTT assay

Cytotoxicity was determined using 3-[4,5-dimethylthiazole-2-yl]-2,5-diphenyltetrazolium bromide (MTT) method. Exponentially growing cells were trypsinized, counted and seeded at the appropriate densities (2000-1000 cells/0.33 cm^2 well) into 96-well microtiter plates. Cells then were incubated in a humidified atmosphere at 37˚C for 24 h. Then, cells were exposed to different concentrations of compounds (0.01, 0.1, 1.0, 10, 100 µM) for 48 h. Then the viability of treated cells was determined using the MTT technique as follow. Media was removed; cells were incubated with 200 µl of 5% MTT solution/well (Sigma Aldrich, MO) and were allowed to metabolize the dye into colored-insoluble formazan crystals for 2 h. The remaining MTT solution was discarded from the wells and the formazan crystals were dissolved in 200 µl/well acidified isopropanol for 30 min, covered with aluminum foil and with continuous shaking at room temperature. The absorbance of each well was measured at a wavelength of 450 nm using a Robonik P2000 EIA reader. The cell viability was expressed as a percentage of control and the concentration that induces 50% of maximum inhibition of cell proliferation (IC_{50}) was determined using Graph Pad Prism software (Graph Pad software Inc, CA) [39,40].

4.2.2. ***Determination of Bax***

Human active Bax content was determined according to DRG® Human Bax ELISA (EIA-4487) kit. PC-3 cells were grown in RPMI 1640 containing 10% fetal bovine serum at 37°C, stimulated with the compounds to be tested for Bax, and lysed with Cell Extraction Buffer. This lysate was diluted in Standard Diluent Buffer over the range of the assay and measured for human active Bax content. (cells are Plated in a density of 1.2 – 1.8 × 10,000 cells/well in a volume of 100µl complete growth medium + 100 ul of the tested compounds per well in a 96-well plate for 24 hours before measuring human Bax).

4.2.3. ***Determination of Bcl-2***

Zymed® Bcl-2 ELISA Kit (Cat. No. 99-0042) was used for determination of Bcl-2 content. PC-3 cells were grown in RPMI 1640 containing 10% fetal bovine serum at 37°C, stimulated with the

compounds to be tested for Bcl-2, and lysed with Cell Extraction Buffer. This lysate was diluted in Standard Diluent Buffer over the range of the assay and measured for human active Bcl-2 contents. (cells are Plated in a density of 1.2 – 1.8 × 10,000 cells/well in a volume of 100µl complete growth medium + 100 ul of the tested compounds per well in a 96-well plate for 24 hours before measuring human Bcl-2).

4.2.4. ***Determination of caspase-3***

PC-3 cells were grown in RPMI 1640 containing 10% fetal bovine serum at 37 °C, stimulated with the compounds to be tested for caspase-3, and lysed with Cell Extraction Buffer. This lysate was diluted in standard diluent buffer over the range of the assay and measured for human active caspase-3 content (cells are plated in a density of 1.2–1.8×10,000 cells/well in a volume of 100 µL complete growth medium+ 100 uL of the tested compound per well in a 96-well plate for 24 h before the enzyme assay) using Invitrogen ELISA Kit (Cat. No. KHO1091).

4.2.5. ***Cell Cycle Analysis*** (DNA-Flow Cytometry Analysis):

PC-3 cells at a density of 4 x106 cells by T 75 flasks were exposed to **4a** at its IC_{50} for 24 h. The cells then were collected by trypsinization, washed in phosphate buffered saline and fixed in ice-cold absolute alcohol. Thereafter, cells were stained using Cycle TEST^{TM} PLUS DNA Reagent Kit (BD Biosciences, San Jose, CA) according to the manufacturer's instructions. Cell-cycle distribution was determined using a FACS Calibur flow cytometer (BD Biosciences, San Jose, CA).

4.2.6. ***Apoptotic analysis***

PC-3 cells were seeded in 24-well tissue culture plates. After 24 h, the medium was changed and **4a** at IC_{50} concentrations were added. After treatment for 48 h, cells floating in the medium were collected. The adherent cells were detached with 0.05% trypsin. Then culture medium having 10% FBS (and floating cells) was added to inactivate trypsin. After gentle pipetting, the cells were centrifuged at 1500 g for 5 min. The supernatant was removed and cells were stained with annexin V-fluorescein isothiocyanate and propidium iodide (PI) according to the manufacturer's instructions. Untreated cells were used as the control for double staining. Immediately after staining the cells, were analyzed by a FACScan flow cytometer.

4.2.7. *Western blotting*

β-actin antibody was purchased from Sigma–Aldrich Chemical Company (Egyptian International Center for Import Cairo, Egypt). Glyceraldehyde 3-phosphate dehydrogenase (GAPDH) was purchased from Santa Cruz Biotechnology, Inc. (Santa Cruz Co., Santa Cruz, CA, USA). Antibodies Poly (ADP-ribose) polymerase (PARP), Bcl-2, Bax, caspase-7, cleaved caspase-7, survivin, horseradish peroxidase-conjugated (HRP) anti-mouse and anti-rabbit secondary antibodies were all obtained from Cell Signaling Technology (Beverly, MA, USA). Mini-protean precast Tris-Glycine gels were from BioRad (Hercules, CA, USA) and the 8.0 μm pore size trans-well membrane inserts was from BD Bioscience (Cat# 353097). All other chemicals were purchased from Sigma-Aldrich (Egyptian International Center for Import Cairo, Egypt) unless otherwise stated.

Protein lysates (approximately 20–30 μg of protein) were denatured in 2X Laemmli sample buffer and subjected to electrophoresis on 8–12% sodium dodecyl sulfate–polyacrylamide gels (SDS-PAGE) or Tris–glycine gels as previously described [41,42]. The separated proteins were transferred onto nitrocellulose membranes followed by blocking with 5% non-fat milk powder (w/v) in Tris-buffered saline (10mM Tris-HCl, pH 7.5, 100mM NaCl, 0.1% Tween 20) for 45 min at room temperature as earlier described [41-43]. Membranes were probed for proteins of interest using specific primary antibodies followed by the appropriate peroxidase-conjugated secondary antibody. The blots were exposed to enhanced chemiluminescence (ECL) and subjected to autoradiography using a BioRad imaging system. To ensure equal protein loading, membranes were stripped and re-probed with appropriate loading controls. Densitometric analyses of the visualized protein bands were performed using the BioRad digitized scientific software program Quantity One. Bands were scanned and processed with Adobe Photoshop CS 6.0 (Adobe Systems, San Jose, CA, USA). Multiple exposures were performed to ensure a linear range of band densities. Three independent experiments were performed for each analysis and protein expression levels were analyzed in triplicate with comparable results. Final data were analyzed by one-way ANOVA.

4.3. *Molecular docking study*

Molecular docking study was done using Molecular Operating Environment (MOE-Dock 2014.09) software [44]. The structures of compounds **I** and **4a** were drawn using the builder

button. Then, these compounds were exposed to energy minimization by utilizing the default MMFF94x force field in the MOE program. Here, low energy 3D conformers of the tested compounds were docked into the active site of surviving protein (PDB code: 3UIH). During the docking process, water molecules were removed. The missing hydrogen atoms were added in order of the correct ionization states to be assigned to the protein structure. "Docking" module in MOE was run to perform the molecular docking. Docking procedure has been applied with default settings. The top 30 poses as ranked by London dG were kept and minimized using MMFF94x within a rigid receptor. The GBVI/WSA dG (Generalized-Born Volume Integral/Weighted Surface area) scoring function was then applied to score the resulting poses. "Ligand Interactions" MOE tool was then used to analyze the molecular docking results by a visualization of the protein–ligand interactions in the active site of the complex. The tool presents in a diagram form an identification and visualization of the interactions between the ligand and the receptor interacting entities, solvent molecules, and ions in the active site of the protein. Among the main interactions included are hydrogen bonds, salt bridges, hydrophobic and cation–π and π –π interactions.

4.4. *Molecular dynamic simulation*

Prior to MD simulations, the complex, in the dimerization interface was minimized stepwise with respect to the force field energy by using the Amber package to attain a low energy conformation. Survivin was described using the Amber Force Field, ligand was described using the Generalized Amber Force Field (GAFF), and the Zinc Amber Force Field (ZAFF) was used. Then the complex was subjected to MD simulations at 300 K during 400 ps. The time step of the simulation was 2.0 fs with a cutoff 10 Å for the non-bonded interactions. The MD simulations are performed at constant temperature and pressure. During the MD simulations all backbone atoms of the surviving were restrained to their starting positions with harmonic force constant 2.0 Kcal/(mol $Å^2$).

This research did not receive any specific grant from funding agencies in the public, commercial, or not-for-profit sectors.

References

1. S. Elmore, Apoptosis: a review of programmed cell death, *Toxicol. Pathol.* 35 (2007) 495–516. http://doi:org/10.1080/01926230701320337
2. Z. N. Oltvai, C. L. Milkman, S. J. Korsmeyer, Bcl-2 heterodimerizes *in vivo* with a conserved homolog, Bax, that accelerates programmed cell death, *Cell* 74 (1993) 609-619. http://doi:org/10.1016/0092-8674(93)90509-o
3. H. W. Findley, L. Gu, A. M. Yeager, M. Zhou, Expression and regulation of Bcl-2, Bcl-xl, and Bax correlate with p53 status and sensitivity to apoptosis in childhood acute lymphoblastic leukemia, *Blood* 89 (1997) 2986-2993. PMID: 9108419
4. D. E. Fisher, Apoptosis in cancer therapy: crossing the threshold, *Cell* 78 (1994) 539. http://doi:org/10.1016/0092-8674(94)90518-5
5. J. F. R. Kerr, C. M. Winterford, B. V. Harmon, Apoptosis. Its significance in cancer and cancer therapy, *Cancer* 73 (1994) 2013–2026. http://doi:org/10.1002/1097-0142(19940415)73
6. C. H. A. Cheung, H. Chen, C. Kuo, C. Chang, M. S. Coumar, H. Hsieh, J. Chang, Survivin counteracts the therapeutic effect of microtubule de-stabilizers by stabilizing tubulin polymers, *Mol. Cancer.* 8 (2009) 43. http://doi:org/10.1186/1476-4598-8-43
7. M. Xiao, W. Li, Recent advances on small-molecule survivin inhibitors, *Curr. Med. Chem.* 9 (2015) 1136–1146. PMID: 25613234
8. S. N. Chettiar, J. V. Cooley, I. Park, D. Bhasin, A. Chakravarti, P. Li, C. Li, N. K. Jacob, Design, synthesis and biological studies of survivin dimerization modulators that prolong mitotic cycle, *Bioorg. Med. Chem. Lett.* 23 (2013) 5429–5433. http://doi:org/10.1016/j.bmcl.2013.07.034.
9. H. Adisetiyo, M. Liang, C. Liao, A. Aycock-Williams, M. B. Cohen, S. Xu, N. Neamati, E. M. Conway, C. Cheng, A. Y. Nikitin, P. Roy-Burman, Loss of survivin in the prostate epithelium impedes carcinogenesis in a mouse model of prostate adenocarcinoma, *PLoS One* 8 (2013) 69484. http://doi:org/10.1371/journal.pone.0069484
10. A. H. Abadi, T. M. Ibrahim, K. M. Abouzid, J. Lehmann, H. N. Tinsley, B. D. Gary, G. A. Piazza, Design, synthesis and biological evaluation of novel pyridine derivatives as anticancer agents and phosphodiesterase 3 inhibitors, *Bioorg. Med. Chem*. 17 (2009) 5974–5982. http://doi:org/10.1016/j.bmc.2009.06.063

11. P. K. Jaiswal, A. Goel, R. D. Mittal, Survivin: A molecular biomarker in cancer, *Indian J. Med. Res*. 141 (2015) 389-397. http://doi:org/10.4103/0971-5916.159250
12. A. Chakravarti, G. G. Zhai, M. Zhang, R. Malhotra, D. E. Latham, M. A. Delaney, P. Robe, U. Nestler, Q. Song, J. Loeffler, Survivin enhances radiation resistance in primary human glioblastoma cells via caspase-independent mechanisms, *Oncogene* 23 (2004) 7494–7506. http://doi:org/10.1038/sj.onc.1208049
13. Q. Wang, K. E. Arnst, Y. Xue, Z. Lei, D. Ma, Z. Chen, D. D. Miller, W. Li, Synthesis and biological evaluation of indole-based UC-112 analogs as potent and selective survivin inhibitors, *Eur. J. Med. Chem.* 149 (2018) 211-224. http://doi:org/10.1016/j.ejmech.2018.02.045
14. X. Liu, R. Gao, Y. Dong, L. Gao, Y. Zhao, L. Zhao, X. Zhao, H. Zhang, Survivin gene silencing sensitizes prostate cancer cells to selenium growth inhibition, *BMC Cancer* 10 (2010) 418. http://doi:org/10.1186/1471-2407-10-418
15. M. K. Abd elhameid, N. Ryad, A. MY, M. R. Mohammed, M. M. Ismail, S. El Meligiea, Design, synthesis and screening of 4, 6-diaryl pyridine and pyrimidine derivatives as potential cytotoxic molecules, *Chem. Pharm. Bull.* 10 (2018) 939-952. http://doi:org/10.1248/cpb.c18-00269
16. A. Malki, M. Mohsen, H. Aziz, O. Rizk, O. Shaaban, M. El-Sayed, Z.A. Sherif , H. Ashour, New 3-cyano-2-substituted pyridines induce apoptosis in MCF 7 breast cancer cells, *Molecules* 21(2016) 230. http://doi:org/10.3390/molecules21020230
17. P. S. Ghosh, K. Manna, U. Banik, M. Das, P. Sarkar, Synthetic strategies and pharmacology of 2-oxo-3-cyanopyridine derivatives, *Int. J. Pharm. Pharm. Sci.* 6 (2014) 39–42.
18. E. M. Flefel, H. S. Abbas, R. E. Abdel Mageid, W. A. Zaghary, Synthesis and cytotoxic effect of some novel 1,2-dihydropyridin-3-carbonitrile and nicotinonitrile derivatives, *Molecules* 21 (2016) 30. http://doi:org/10.3390/molecules21010030
19. I. Abbas, S. Gomha, M. Elaasser, M. Bauomi, Synthesis and biological evaluation of new pyridines containing imidazole moiety as antimicrobial and anticancer agents, *Turk. J. Chem.* 39 (2015) 334- 346. http://doi:org/10.3906/kim-1410-25
20. M. A. O. Abdelf-Fattah, M. A. M. El-Naggar, R. M. H. Rashied, B. D. Gary, G. A. Piazza, A. H. Abadi, Four-component synthesis of 1,2-dihydropyridine derivatives and their evaluation as anticancer agents, *Med. Chem.* 8 (2012) 392–400. PMID: 22530887

21. M. F. Harras, R. Sabour, Design, synthesis and biological evaluation of novel 1,3,4-trisubstituted pyrazole derivatives as potential chemotherapeutic agents for hepatocellular carcinoma. *Bioorg. Chem.* 78 (2018) 149-157. http://doi.org/10.1016/j.bioorg.2018.03.014
22. M. E. Abdelaziz, M. M. M. El-Miligy, S. M. Fahmy, M. A. Mahran, A. A. Hazzaa, Design, synthesis and docking study of pyridine and thieno[2,3-b] pyridine derivatives as anticancer PIM-1 kinase inhibitors, *Bioorg. Chem.* 80 (2018) 674-692. https://doi.org/10.1016/j.bioorg.2018.07.024
23. F. M. A. Altalbawy, Synthesis and antimicrobial evaluation of some novel bis-α,β-unsaturated ketones, nicotinonitrile, 1,2-dihydropyridine-3-carbonitrile, fused thieno[2,3-b]pyridine and pyrazolo[3,4-b]pyridine derivatives, *Int. J. Mol. Sci.* 14 (2013) 2967-2979. http://doi.org/10.3390/ijms14022967
24. J. M. Golbano, P. Lopez-Aparicio, M. N. Recio, M. A. Perez-Albarsanz, Finasteride induces apoptosis via Bcl-2, Bcl-xL, Bax and caspase-3 proteins in LNCaP human prostate cancer cell line, *Int. J. Onc.* 32 (2008) 919-924. PMID: 18360719
25. I. Dolka, M. Kr´ol, R. Sapierzy´nski, Evaluation of apoptosis-associated protein (Bcl-2, Bax, cleaved caspase-3 and p53) expression in canine mammary tumors: An immunohistochemical and prognostic study, *Res. Vet. Sci.* 105 (2016) 124-133. http://doi.org/10.1016/j.rvsc.2016.02.004
26. D. G. Tang, A. T. Porter, Target to apoptosis: a hopeful weapon for prostate cancer. *Prostate* 32 (1997) 284-293. PMID: 9288188
27. S. Jin, Y. Yang, L. Ma, B. Ma, L. Ren, L. Guo, W. Wang, Y. Zhang, Z. Zhao, M. Cui, *In vivo* and *in vitro* induction of the apoptotic effects of oxysophoridine on colorectal cancer cells via the Bcl-2/Bax/caspase-3 signaling pathway, *Oncol. Lett.* 14 (2017) 8000-8006. 2017. http://doi.org/10.3892/ol.2017.7227
28. K. T. Chan, F. Y. Meng, Q. Li, C. Y. Ho, T. S. Lam, Y. To, W. H. Lee, M. Li, K. H. Ch, M. Toh, Cucurbitacin B induces apoptosis and S phase cell cycle arrest in BEL-7402 human hepatocellular carcinoma cells and is effective via oral administration, *Cancer Lett.* 294 (2010) 118-124. http://doi.org/10.1016/j.canlet.2010.01.029.
29. J. K. Shen, H. P. Du, M. Yang, Y. G. Wang, J. Jin, Casticin induces leukemic cell death through apoptosis and mitotic catastrophe, *Ann. Hematol.* 88 (2009) 743-752. http://doi.org/10.1007/s00277-008-0677-3.

30. V. G. Reddy, T. S. Reddy, V. L. Nayak, B. Prasad, A. P. Reddy, A. Ravikumar, S. Taj, A. Kamal, Design, synthesis and biological evaluation of N-((1-benzyl-1H-1,2,3-triazol-4-yl)methyl)-1,3-diphenyl-1H-pyrazole-4-carboxamides as CDK1/Cdc2 inhibitors, *Eur. J. Med. Chem.* 122 (2016) 164-177. http://doi.org/10.1016/j.ejmech.2016.06.011
31. Q. Wei, J. Li, F. Tang, Y. Yin, Y. Zhao, Q. Yao, Synthesis and biological evaluation of novel 2-arylvinyl-substituted naphtho[2,3-d]imidazolium halide derivatives as poten antitumor agents, *Eur. J. Med. Chem.* 144 (2018) 504-516. http://doi.org/10.1016/j.ejmech.2017.12.008.
32. H. Boulares, A. G. Yakovlev, V. Ivanova, B.A. Stoica, G. Wang, S. Iyer, M. Smulson, Role of Poly(ADP-ribose) Polymerase (PARP) cleavage in apoptosis, *J. Biol. Chem.* 274 (1999) 22932–22940. PMID: 10438458
33. B. Zhang, N. Wang, C. Zhang, C. Gao, W. Zhang, K. Chen, W. Wu, Y. Chen, C. Tan, F. Liu, Y. Jiang, Novel multi-substituted benzyl acridone derivatives as survivin inhibitors for hepatocellular carcinoma treatment, *Eur. J. Med. Chem.* 129 (2017) 337-348. http://doi.org/10.1016/j.ejmech.2017.02.027
34. J. Qi, Z. Dong, J. Liu, RC. Peery, S. Zhang, JY. Liu, JT. Zhang, Effective targeting of the survivin dimerization interface with small-molecule inhibitors, *Cancer Res.* 76 (2016) 453-462. http://doi.org/ 10.1158/0008-5472.CAN-15-1874
35. L. Chantalat, DA. Skoufias, JP. Kleman, B. Jung, O. Dideberg, RL. Margolis, Crystal structure of human survivin reveals a bow tie-shaped dimer with two unusual alpha-helical extensions, *Mol. Cell*. 6 (2000) 183-9. PMID:10949039
36. X. Alejandro, Dominguez, B. Gomez, E. Homberag, J. Slim, Studies on bis-(benzylisoquinolines). I. Synthesis of dl-N-(4-hydroxyphenylacetyl)-5-iodo-4-acetoxy-3-methoxyphenyl alanine methyl ester, *J. Amer. Chem. Soc*. 77 (1955) 1288-1290.
37. S. Iftikhar, S. Khan, A. Bilal, S. Manzoor, M. Abdullah, A. Emwas, S. Sioud, X. Gao, G. A. Chotana, A. Faisal, R. S. Z. Saleem, Synthesis and evaluation of modified chalcone based p53 stabilizing Agents, *Bioorg. Med. Chem. Lett.* 27 (2017) 4101–4106. http://doi.org/10.1016/j.bmcl.2017.07.042
38. K. C. Gautam, D. P. Singh, Synthesis and antimicrobial activity of some isoxazole derivatives of thiophene, *Chem. Sci. Trans.* 2 (2013) 992-996. http://doi.org/10.7598/cst2013.478

39. T. Mosmann, Rapid colorimetric assay for cellular growth and survival: application to proliferation and cytotoxicity assays, *J. Immunol. Methods* 65 (1983) 55-63. http://doi:org/10.1016/0022-1759(83)90303-4

40. D. A. Scudiero, D. A. Scudiero, R. H. Shoemaker, K. D. Paull, A. Monks, S. Tierney, T. H. Nofziger, M. J. Currens, D. Seniff, M. R. Boyd, Evaluation of a soluble tetrazolium/formazan assay for cell growth and drug sensitivity in culture using human and other tumor cell lines, *Cancer Res*. 48 (1988) 4827-4833. PMID: 3409223

41. J. C. Chamcheu, F. Afaq, D. N. Syed, I. A. Siddiqui, V. M. Adhami, N. Khan, S. Singh, B. T. Boylan, G. S. Wood, H. Mukhtar, Delphinidin, a dietary antioxidant, induces human epidermal keratinocyte differentiation but not apoptosis: Studies in submerged and three-dimensional epidermal equivalent models, *Exp. Dermatol.* 22 (2013) 342–348. http://doi:org/10.1111/exd.12140

42. J. C. Chamcheu, E. P. Lorie, B. Akgul, E. Bannbers, M. Virtanen, L. Gammon, A. Moustakas, H. Navsaria, A. Vahlquist, H. Torma, Characterization of immortalized human epidermolysis bullosa simplex (KRT5) cell lines: Trimethylamine N-oxide protects the keratin cytoskeleton against disruptive stress condition. *J. Dermatol. Sci.* 53 (2009) 198–206. http://doi:org/10.1016/j.jdermsci.2008.11.003

43. J. C. Chamcheu, V. M. Adhami, S. Esnault, M. Sechi, I. A. Siddiqui, K. A. Satyshur, D. N. Syed, S. M. Dodwad, M. I. Chaves-Rodriquez, B. J. Longley, G. S. Wood, H. Mukhtar, Dual Inhibition of PI3K/Akt and mTOR by the Dietary Antioxidant, Delphinidin, Ameliorates Psoriatic Features In Vitro and in an Imiquimod-Induced Psoriasis-Like Disease in Mice. Antioxid. Redox Signal. 26 (2017) 49–69. http://doi:org/10.1089/ars.2016.6769

44. Molecular Operating Environment (MOE) 2014.09, Chemical Computing Group Inc., 1010 Sherbrooke Street West, Suite 910, Montréal, H3A 2R7, Canada, http://www.chemcomp.com

Table 1. Cytotoxicity of compounds **4-6** and 5-FU evaluated in different human cancer cells [a].

Compound	IC_{50} (μM)		
	PC-3	**HepG2**	**MDA-MB-231**
4a	0.42±0.05	1.22±0.06	0.66±0.03
4b	1.45±0.12	3.53±0.28	2.16±0.23
4c	9.83±0.97	14.61±1.20	12.82±1.60
4d	7.12±0.81	12.62±1.10	9.16±0.94
5a	14.71±1.3	21.35±1.30	18.38±1.07
5b	4.97±0.46	12.51±1.10	8.68±0.85
5c	1.62±0.09	3.64±0.32	3.32±0.27
5d	6.95±0.58	13.17±0.98	10.71±1.01
6a	6.31±0.51	10.64±0.95	8.22±0.76
6b	2.41±0.30	6.92±0.68	4.72±0.41
6c	1.72±0.11	3.91±0.25	2.83±0.15
6d	7.42±0.64	11.52±0.97	9.34±0.85
5-FU	7.53±0.09	8.15±0.11	9.35±0.74

[a] The inhibitory effects of compounds on the cancer cell lines were determined by the MTT assay. The data are expressed as the mean ± SD of three independent experiments.

Table 2. IC_{50} values of compounds **4a, 4b, 5c** and **6c** on the normal WI-38 cell line [a].

Compound	**4a**	**4b**	**5c**	**6c**
WI-38 IC_{50} (µM)	193.15±0.09	193.64±0.11	169.32±0.68	148.57±0.12

[a] The inhibitory effects of compounds on the normal WI-38 cell line were determined by the MTT assay. The data are expressed as the mean ± SD of three independent experiments.

Table 3. Effect of compounds **4a, 4b, 5c** and **6c** on the level of some apoptosis key markers [a].

Compound	Bcl-2 (ng/ml)	Bax (ng/ml)	Caspase-3 (Pg/ml)
4a	1.44±0.27	301.0±0.10	393.6±0.32
4b	2.43±0.25	244.3±0.09	336.7±0.22
5c	1.67±0.30	263.8±0.78	346.7±0.19
6c	2.82±0.25	208.9±0.11	329.1±0.11
Control	5.60±0.16	33.9±0.08	46.2±0.15

[a] The effects of **4a, 4b, 5c** and **6c** on the amount of Bcl-2, Bax and Caspase-3 were determined after 24 h using ELISA Kits. The data are expressed as the mean ± SD of three independent experiments

Table 4. Docking parameters for compounds **I** and **4a** with survivin.

Compound	Docking score ΔG (kcal/mol)	Atoms and amino acids involved in the interaction	Type of interaction	Distance (A^0)
I	-6.790	Pyridine N ….. Gln 92 Hydroxyl O ….. Glu 40 4-Phenyl ring ….. Arg 18	H-bond H-bond Pi-H	2.55 3.25 3.83
4a	-8.478	Amino N …. Glu 40 Cyano N …. Lys 15 Cyano N …. Arg 18 4-Phenyl ring …. Phe 93	H-bond H-bond H-bond Pi-cation	3.15 2.84 3.63 3.87

Table 5. The interactions involved at the dimerization interface of the wild-type and the complex-type.

Dimer type	H-bonding interactions	Aromatic stacking interactions	Hydrophobic interactions
Wild-type	Thr5 and Asp105	Trp10 and Phe101	Phe93 and Leu98
Complex-type	Ala9, Trp10, Phe58, Asp105, and Arg108	1. Trp10 and Phe101 disrupted 2. Ligand with Phe58	1. Ligand with Phe93 2. Ligand with Leu96 and Phe101

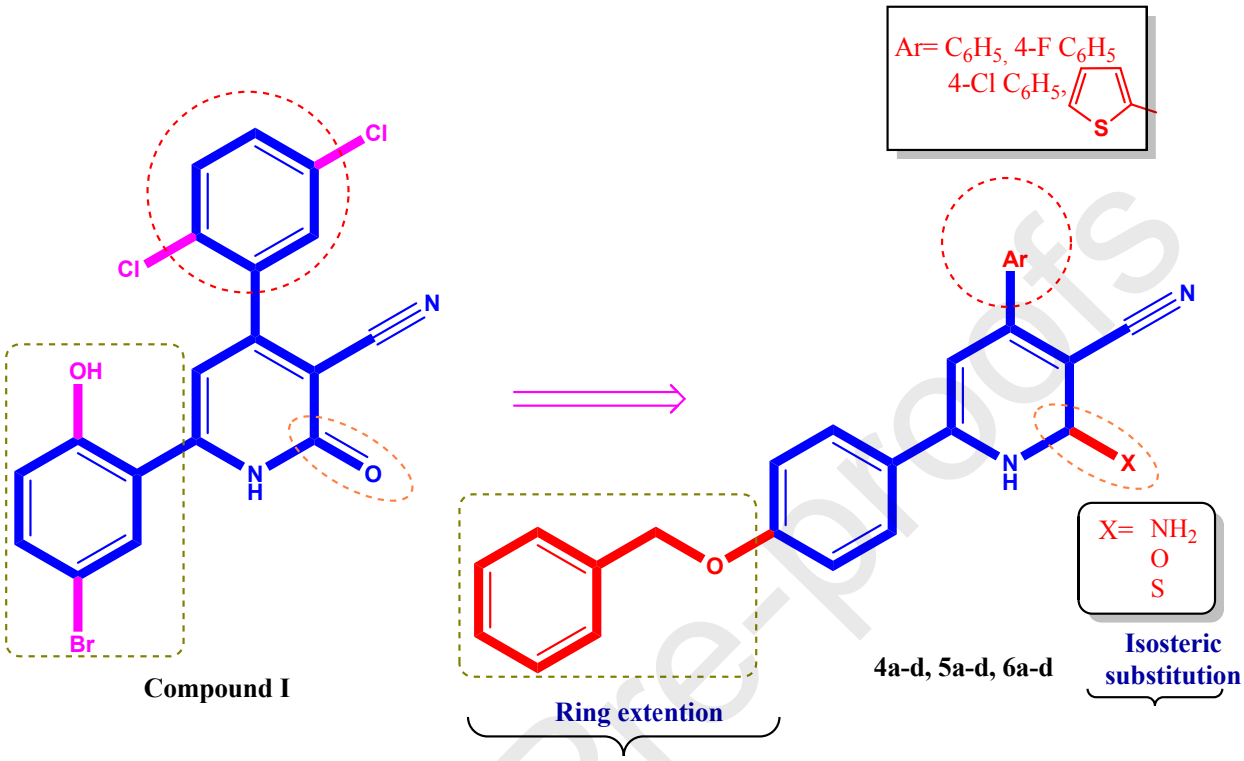

Fig. 1. Compound **I** and structure-based design of 3-cyanopyridine derivatives **4a-d**, **5a-d** and **6a-d** as survivin inhibitors.

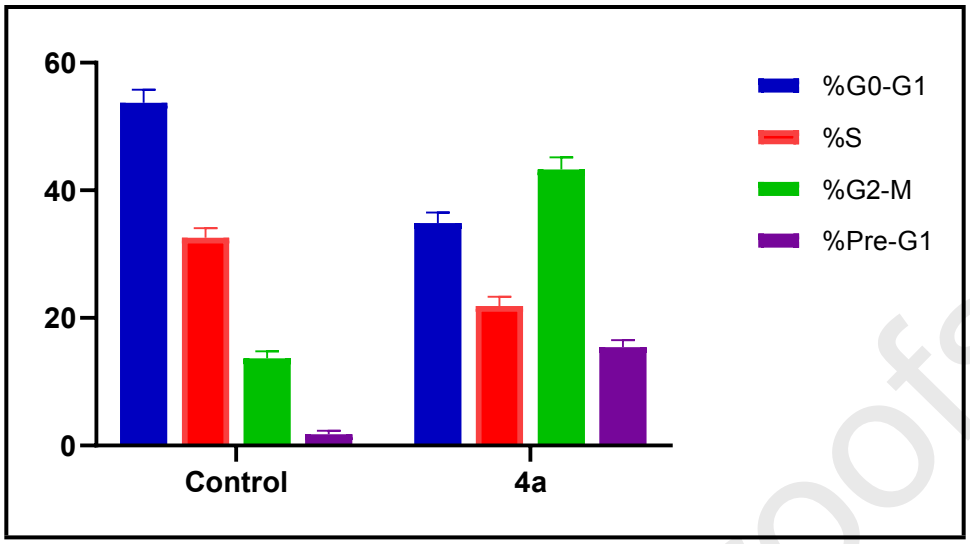

Fig. 2. Cell cycle analysis of PC-3 cells after treatment with **4a** and DMSO control. The data are expressed as the mean ± SD of three independent experiments. The statistical significance was assessed by two-way ANOVA ($P < 0.0001$) in comparison to control.

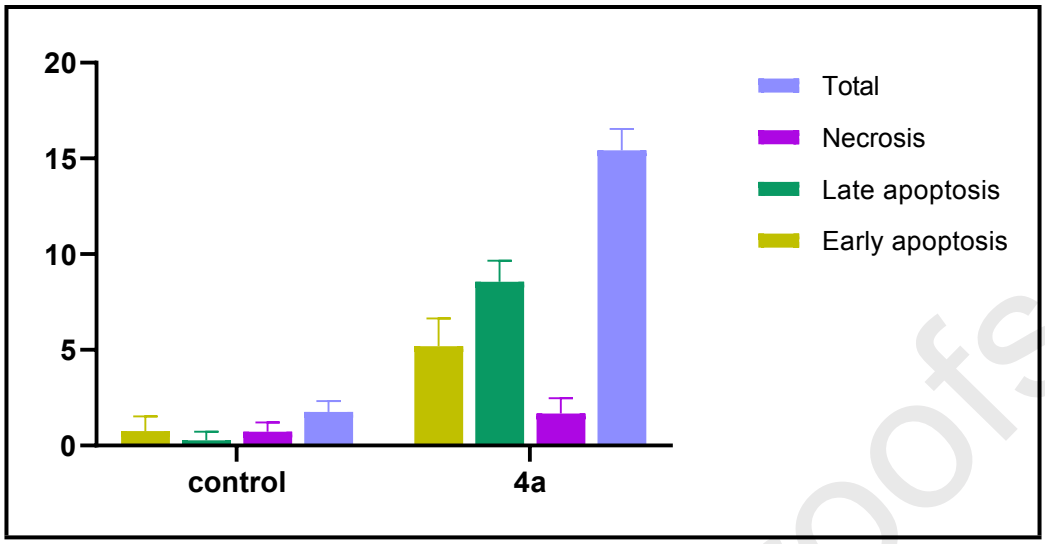

Fig. 3. The percentage of apoptosis and necrosis caused by **4a** using PC-3 cell line. The data are expressed as the mean± SD of three independent experiments. The statistical significance was assessed by two-way ANOVA ($P < 0.0001$) in comparison to control.

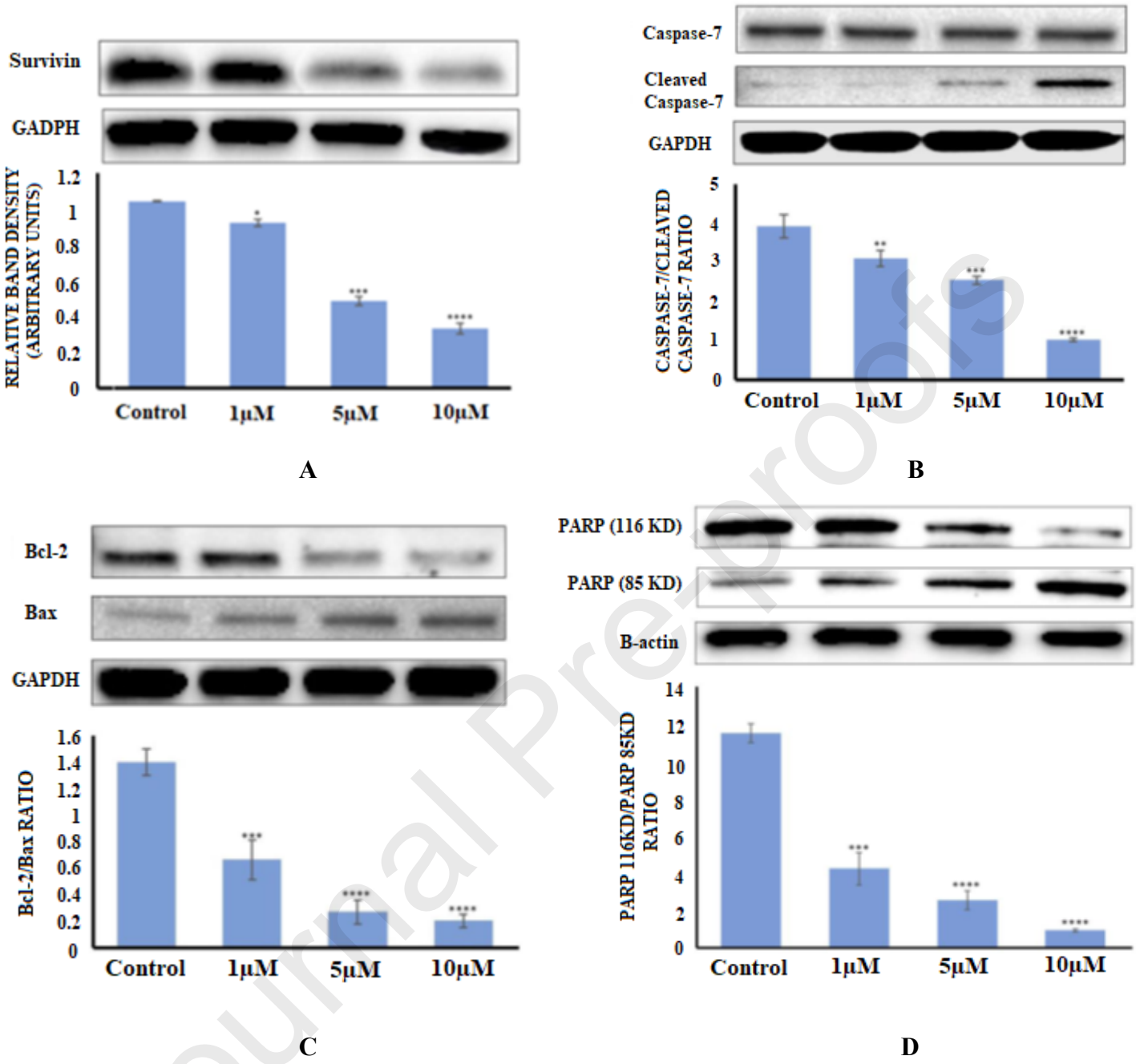

Figs. 4. (**A-D**) Western blotting analysis showed the effect of the different concentration of **4a** on survivin, caspase-7, Bcl-2, Bax and PARP proteins levels respectively, in PC-3 cell using GAPDH/β-actin as loading control.

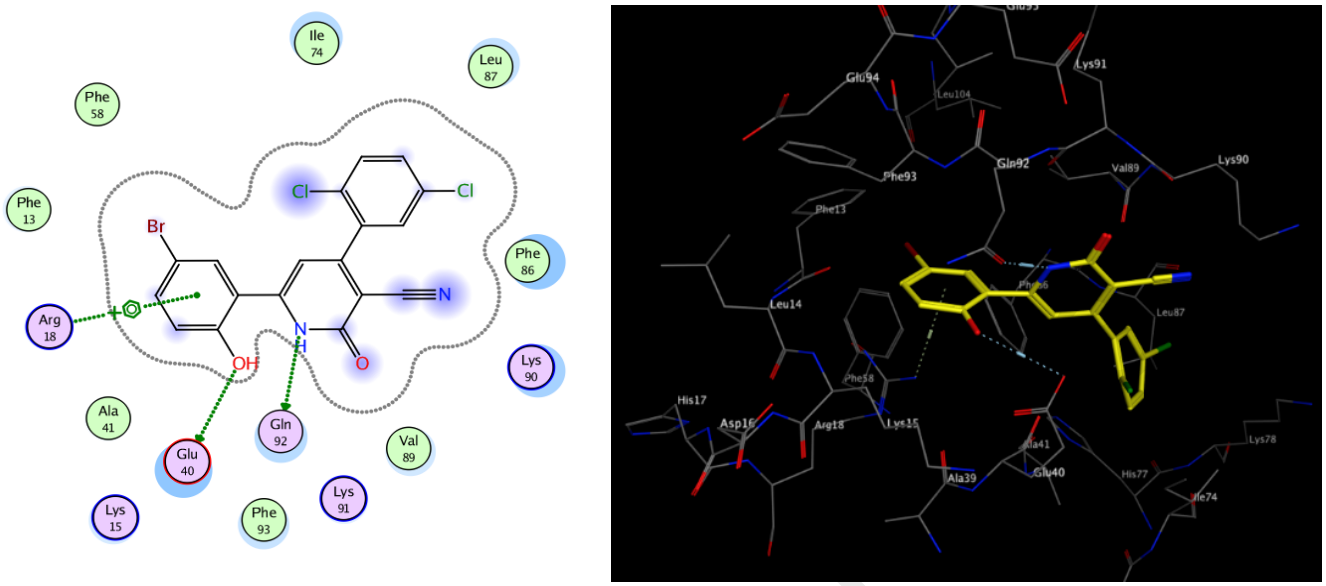

A **B**

Fig. 5. The proposed binding mode of compound **I** docked in the active site of survivin; A and B showing 2D and 3D ligand-receptor interactions.

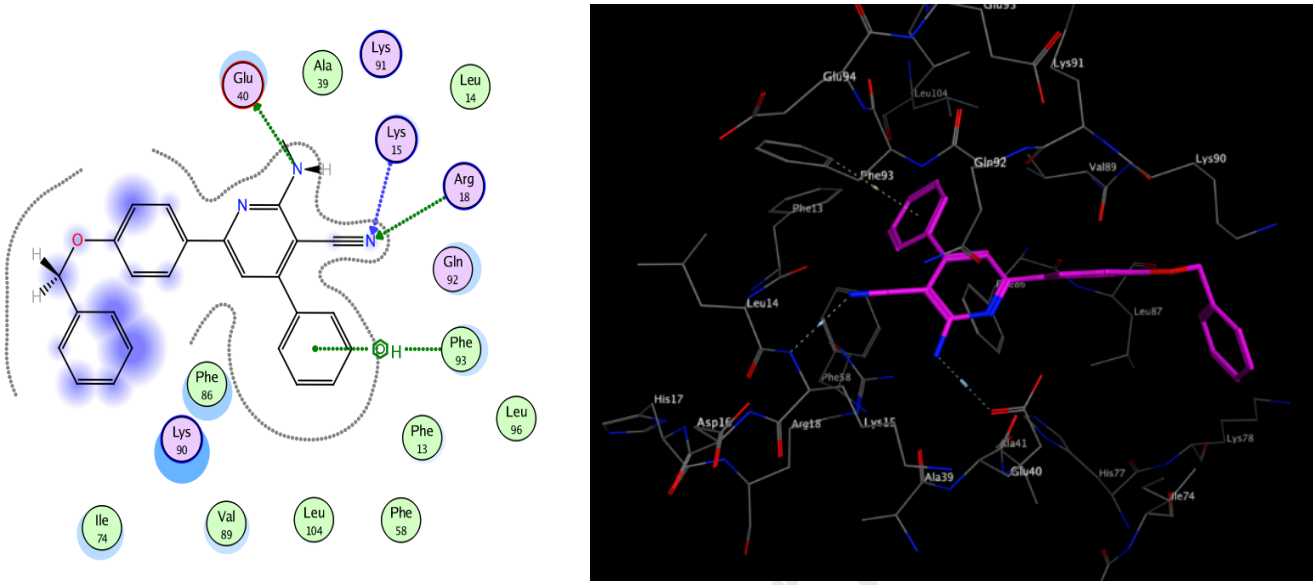

A **B**

Fig. 6. The proposed binding mode of **4a** docked in the active site of survivin; A and B showing 2D and 3D ligand-receptor interactions.

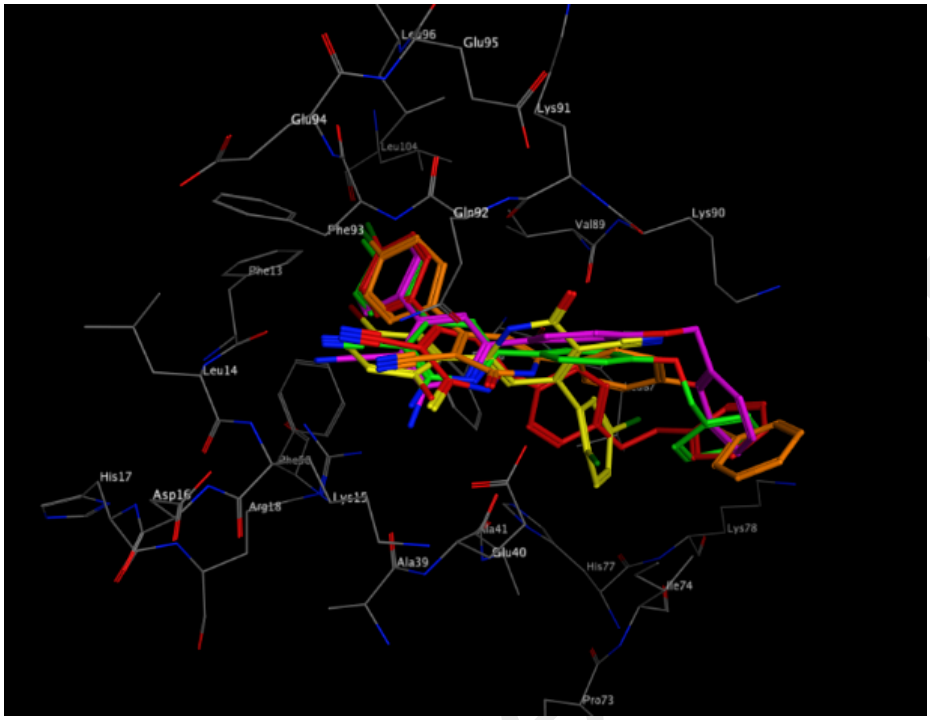

Fig. 7. 3D structure overlapping between **I** (in yellow), **4a** (in purple), **4b** (in green), **5c** (in orange) and **6c** (in red) compounds inside survivin active site.

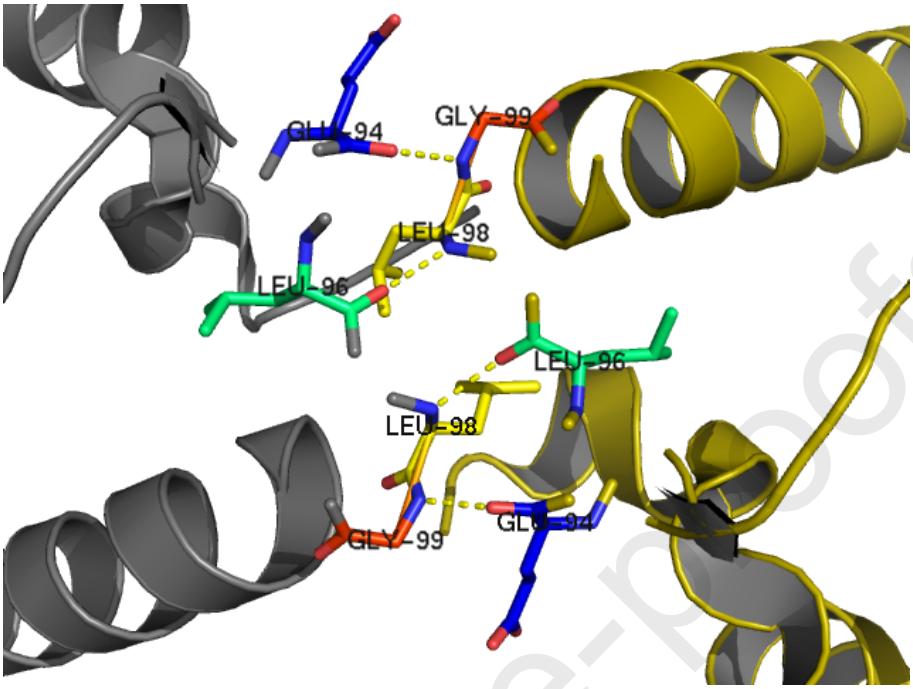

Fig. 8. Backbone hydrogen bonding interactions between chain A (grey) and chain B (olive)

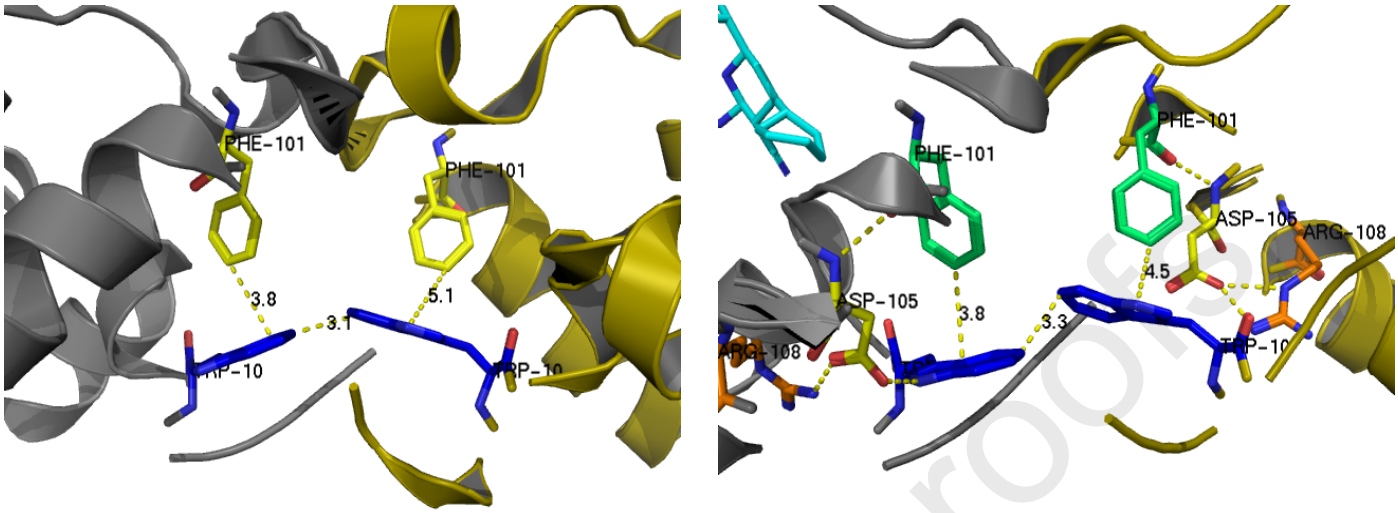

Fig. 9. Aromatic stacking network mediating interactions between chain A (grey) and chain B (olive) wild-type (left) and complex (right)

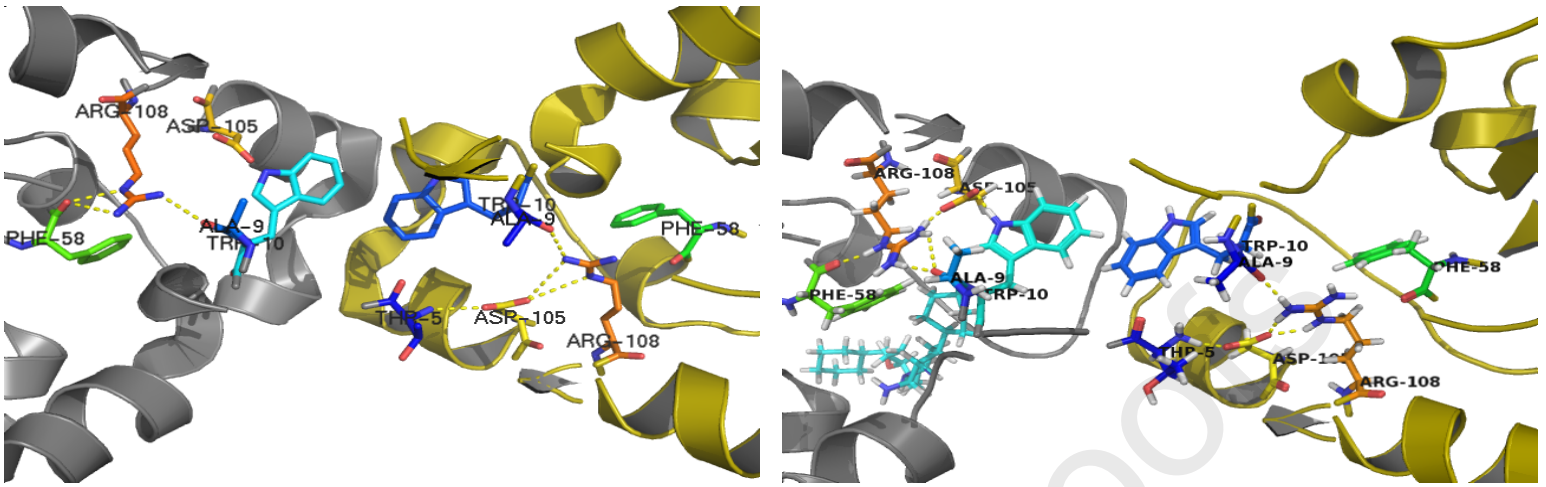

Fig. 10. Hydrogen bonding network mediating interactions. Chain A (grey) and chain B (olive) wild-type (left) and complex (right)

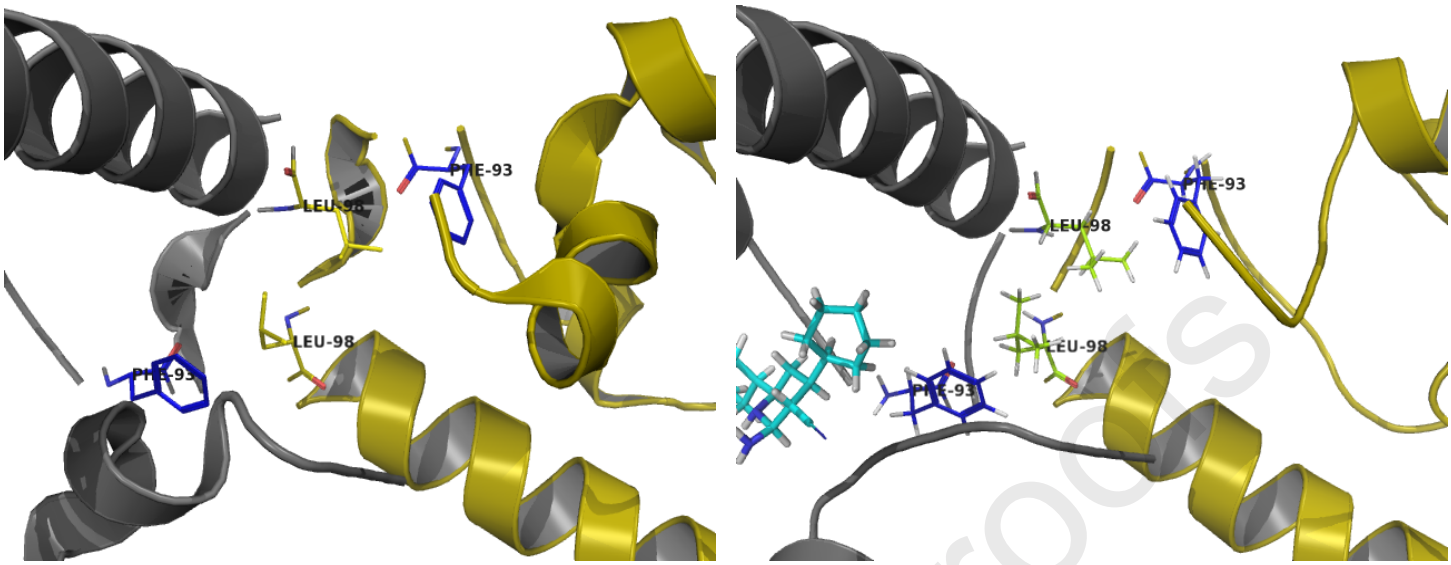

Fig. 11. Hydrophobic interactions between chain A (grey) and chain B (olive) wild-type (left) and complex (right)

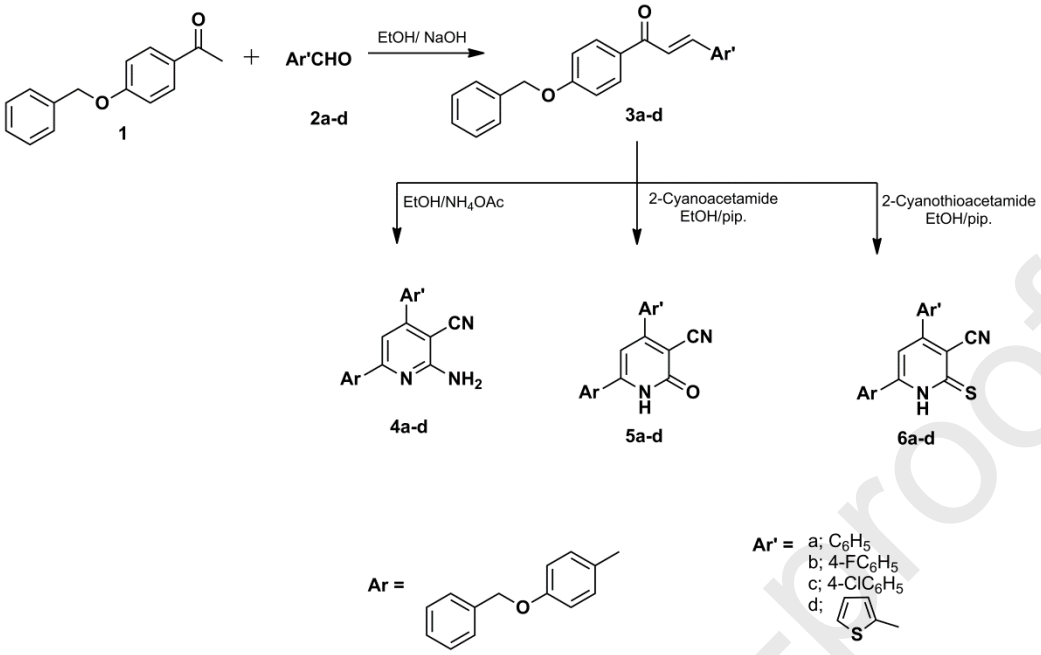

Scheme 1. Synthetic pathway of compounds **4a-d**, **5a-d** and **6a-d**

Conflict of Interest
The authors confirm that this article content has no conflicts of interest

GA

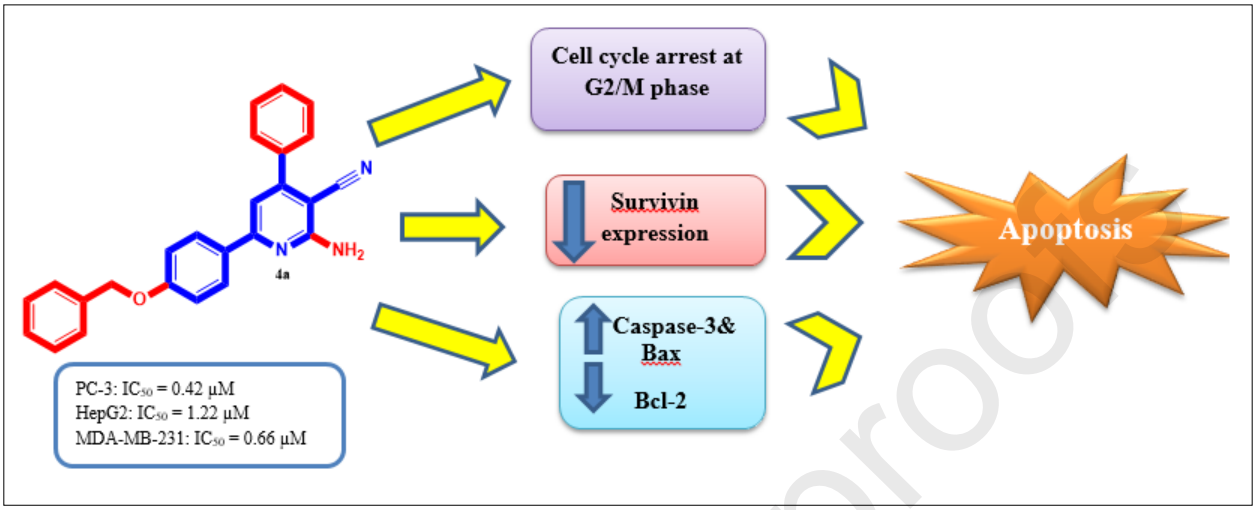

Highlights

- A series of new 3-cyanopyridine derivatives were designed and synthesized.
- Cytotoxic activity was evaluated against PC-3, HepG2 and MDA-MB-231 cell lines.
- Compounds **4a, 4b, 5c** and **6c** elevated Bax, caspase-3 levels and decreased Bcl-2 level.
- Western blotting showed that **4a** markedly inhibited survivin expression in PC-3 cells.
- Molecular docking was performed against survivin.